Theoretical Flow Instability of the Kármán Boundary Layer

Young-Kyu Hwang*, Yun-Yong Lee
School of Mechanical Engineering, Sungkyunkwan University

The hydrodynamic stability of the Kármán boundary-layer flow due to a rotating disk has been numerically investigated for moving disturbance waves. The disturbed flow over a rotating disk can lead to transition at much lower Re than that of the well-known Type I instability mode. This early transition is due to the excitation of the Type II instability mode of moving disturbances. Presented are the neutral stability results concerning the two instability modes by solving new linear stability equations reformulated not only by considering whole convective terms but by correcting some errors in the previous stability equations. The reformulated stability equations are slightly different with the previous ones. However, the present neutral stability results are considerably different with the previously known ones. It is found that the flow is always stable for a disturbance whose dimensionless wave number k is greater than 0.75.

Key Words : Kármán Boundary-Layer Flow, Hydrodynamic Stability, Rotating Disk, Moving Disturbance Wave

1. Introduction

The hydrodynamic stability over a rotating system has been investigated by many scientists to understand the fundamental mechanism of 3-dimensional boundary-layer transition process (Wilkinson and Malik, 1985; Faller, 1991; Kohama and Suda, 1993; Lingwood, 1997). Various types of flows belong to this category. As an example, the stability and transition of rotating flows have been related to weather, typhoons, tornadoes, and similar phenomena over swept-back airfoils such as an impeller, transition process of ICBM's cone, and head levitation process over a HDD.

The rotation of flow system dramatically affects the stability characteristics of flows at various physical situations. After the famous exact solution for the Kármán boundary-layer flow were obtained by Sparrow and Gregg (1960), the progress in the stability theory and experiment for rotating flows has been explosive in the past decades. The stability analysis of Lilly (1966) for the Ekman layer flow revealed that the inclusion of Coriolis term in the stability analysis for stationary disturbance wave yields the significant increment of the critical Reynolds number, $Re_{c,1}$ (*i.e.*, Type I instability). Also, he found that another mode of instability (*i.e.*, Type II instability) for moving disturbance waves, caused by the Coriolis force, exists at much lower value of critical Reynolds number $Re_{c,2}$, compared to those of stationary disturbance waves.

Some examples of the stationary disturbances concerning the Type I instability are described as below.

The Kármán boundary-layer transition on a rotating disk was first studied by Smith (1947) using the hot-wire technique. He observed that some sinusoidal disturbances appeared in the disk boundary-layer at sufficiently large Reynolds numbers. Approximately 32 oscillations were observed within a disk rotation period and his numerical analysis indicated that the disturbances propagated at an angle of about 14° relative to the outward drawn radius (where the direction of

* Corresponding Author,
E-mail : ykhwang@yurim.skku.ac.kr
TEL : +82-331-290-7437 ; **FAX** : +82-331-290-5849
School of Mechanical Engineering, Sungkyunkwan University, Suwon 440-746, Korea. (Manuscript **Received** August 27, 1999; **Revised** December 27, 1999)

disk rotation defines positive angle). Later, Gregory *et al.* (1955) observed 28-31 spiraling outward vortices over a rotating disk at an angle of about 14° by using the china-clay technique for flow visualization. These vortices, which appeared stationary relative to a disk, were first observed at the local Reynolds number $Re \simeq 430$, transition to turbulence occurred at $Re \simeq 530$ (see, also, Gregory and Walker, 1960).

The stationary disturbance wave established in a rotating disk was subsequently studied by lots of investigators mentioned as follow. Kobayashi *et al.* (1980) performed a theoretical analysis in which some of the effects of Coriolis and streamline curvature were considered. They calculated the value of $Re_{c,1}$ as 261 and observed that the number of spiral vortices was 31 or 32 at the position of $Re \simeq 297$ and that the gradient of vortex axis decreased from 14° to 7° as Re was increased. Malik *et al.* (1981) numerically predicted that the critical Reynolds number $Re_{c,1}$, for establishment of stationary disturbance wave is 287 and these vortices spiral outward at an angle of about $\varepsilon_{c,1} = 11.2°$ (Note that the recalculated values of Malik (1986) are $Re_{c,1} = 285.36$ and $\varepsilon_{c,1} = 11.4°$). They observed that there were about 21 vortices at $Re \simeq 294$. Their calculated the value of $Re_{c,2}$ for Type Ⅱ moving disturbance wave was about 49. Faller (1991) considered the effects of Coriolis force and streamline curvature in his stability analysis and obtained the neutral stability results, *e.g.*, $Re_{c,I} = 285.3$, $k_{c,1}$ (wave number at $Re_{c,1}$) $= 0.378$ and $\varepsilon_{c,1}$ (azimuth angle at $Re_{c,1}$) $= 13.9°$ for Type I instability, while $Re_{c,2} = 69.4$, $k_{c,2} = 0.279$, and $\varepsilon_{c,2} = -19.0°$ for Type Ⅱ instability.

For the Kármán boundary-layer flow, Faller (1991) took sequential photographs of dye bands which were moving outward, as seen in Fig. 1(a). The resulting sketches of die patterns in Fig. 1(b) illustrated the typical structures of Type Ⅱ and secondary instabilities.

The present study is a stability analysis of rotating disk flow, (*i.e.*, the Kármán boundary-layer) in which the effects of Coriolis force and streamline curvature are included. The previously known linear stability equations of Faller (1991) are reformulated by correcting sign error and by keeping whole convective terms. The reformulated stability equations are accurately solved by using the orthogonal collocation technique. The results yield more complete 4-dimensional neutral stability curves, corresponding to the Type Ⅰ and Ⅱ instabilities, than those of previous investigators. It will be seen that the flow is always stable for a disturbance whose dimensionless

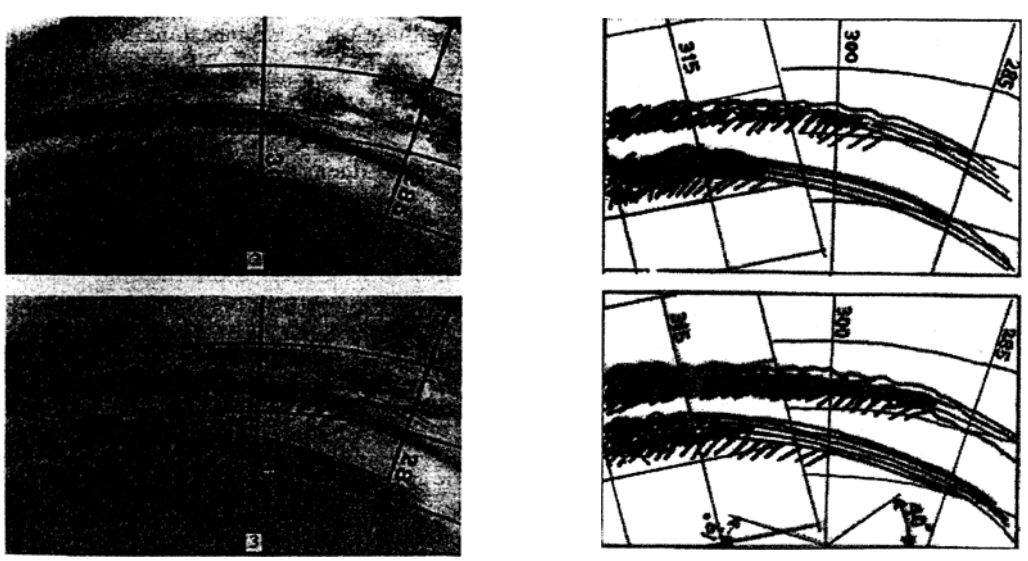

(a) Photo from Faller (1991) (b) Sketch of their structured

Fig. 1 Type Ⅱ and secondary instability of Kármán boundary layer illustrate:

wave number k is greater than 0.75 (*i.e.*, if $\omega_D=$ 0.325 rps, and whose corresponding physical wave number $\bar{k}>4.27\text{cm}^{-1}$). It will also be shown that the azimuth angle of disturbance wave which spiral outward tend to be decreased from 13.2° to lower angle as the local Reynolds number is further increased from $Re_{c,l}$.

2. The Governing Equations

2.1 Base flow equation

The steady, laminar, axi-symmetric flow of an incompressible viscous liquid, which occupies the semi-infinite region on one side of a rotating infinite disk, was first discussed by von Kármán (1921). The similarity equations for the steady laminar base flow of Kármán boundary-layer (with the rotation system in Fig. 3) are well known; for example, Faller (1991). To formulate them the following quantities were used: z (dimensionless axial coordinate), D (a characteristic boundary-layer depth), and $\Delta\omega$ (a relative angular speed of fluid ω_F with respect to the disk ω_D), where

$$z=\frac{\bar{z}}{D},\ D=\left(\frac{\nu}{\omega_D}\right)^{\frac{1}{2}},\ \Delta\omega=-\omega_D \tag{1}$$

Assuming an axi-symmetrical similarity solution to the base flow with the dimensionless velocities of x, y, z components $F(z)$, $G(z)$, and $H(z)$ defined by

$$U=\Delta\omega rF,\ V=\Delta\omega rG,\ W=\Delta\omega DH \tag{2}$$

and scaling lengths by D and time by rotational disk speed ω_D^{-1}, the radial and tangential base flow equations are

$$F^2+HF_z-(G^2-1)+2(G-1)+F_{zz}=0, \tag{3a}$$

$$2FG+HG_z-2F+G_{zz}=0 \tag{3b}$$

The continuity equation is

$$H=-2\int_0^z F(z')\,dz' \tag{4}$$

The boundary conditions are

$$F(0)=G(0)=H(0)=0,$$
$$F(\infty)=0,\ G(\infty)=1 \tag{5}$$

The boundary-value problem (3a, b)-(5) was solved on the interval $[0,\ \eta_\infty]$ with $\eta_\infty=40-120$. Namely, the base flow solution was crudely obtained first by using a finite difference method (FDM). Then, a computing code COLNEW (Bader and Ascher, 1985) which was designed to solve two-point boundary-value problems accurately, was utilized to find more accurate numerical solution. At that time, the crude solution was used to provide the initial guess for COLNEW. The resulting solutions are stored as B-spline coefficients in order to be called during the stability computation. Nondimensional velocity distribution for the base flow is shown in Fig. 2. Note that the radial base flow direction is negative.

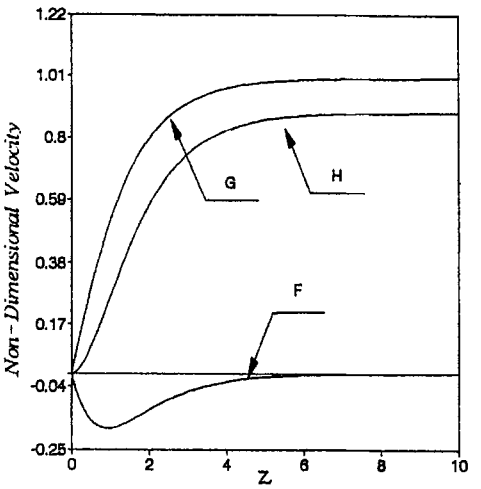

Fig. 2 Numerical solution of base flow equations for Ro$=-1$, Co$=2$

2.2 The linear stability equations

The instability problem of the Kármán boundary-layer has long been a prototype for studies of instabilities in general 3-dimensional boundary-layers. Gregory *et al.* (1955) discussed the application of the swept-back airfoils, and developed a partial theory showing that those waves were associated with an inflection point in the cross-vortex base flow.

The linear stability equations for the Kármán boundary-layer can be derived and reduced to the similarity form as was done by Faller *et al.* (1989) (see, also, Faller, 1991). We follow the way of Faller to reformulate the stability equa-

tions as below. But, our stability equations are slightly different compared to those of Faller. Namely, the present stability equations have been reformulated not only by correcting some errors but by keeping convective terms, instead of neglecting the perturbated terms with respect to r. Both the errors and neglected terms are appeared in the Eq. (30) of Faller *et al.* (1989).

Nondimensional perturbation equations can be formulated by subtracting base flow equations from the r, θ, z components of motion in a cylindrical coordinate system rotating with the angular speed ω_D, by omitting products of fluctuations, and, finally, by introducing the transformations

$$(\bar{u},\ \bar{v},\ \bar{w}) \rightarrow \Delta\omega D(u,\ v,\ w),$$
$$(\bar{r},\ \bar{z}) \rightarrow D(r,\ z),\ \bar{t} \rightarrow t/\omega_D,\ \bar{p} \rightarrow \Delta\omega D^2 p \tag{6}$$

where the value of — means dimensional variable. The non-dimensional perturbation equations are then

$$u_t + Re\left(Fu_r + \frac{Gu_\theta}{r} + wF_z\right) + Ro(Hu_z + Fu - 2Gv) - Cov = -p_r + \nabla^2 u - \frac{u}{r^2} - \frac{2v_\theta}{r^2} \tag{7a}$$

$$v_t + Re\left(Fv_r + \frac{Gv_\theta}{r} + wG_z\right) + Ro(Hv_z + Fv + 2Gu) + Cou = -\frac{p_\theta}{r} + \nabla^2 v - \frac{v}{r^2} + \frac{2u_\theta}{r^2} \tag{7b}$$

$$w_t + Re\left(Fw_r + \frac{Gw_\theta}{r}\right) + Ro(Hw_z + wH_z) = -P_z + \nabla^2 w \tag{7c}$$

$$\frac{(ru)_r}{r} + \frac{v_\theta}{r} + w_z = 0 \tag{7d}$$

where Re is defined as $Re = \Delta\omega \bar{r}\ D/\nu$, $Ro = -1$ and $Co = 2$.

The radial and tangential components of perturbation vorticity equations are denoted as ξ and η

$$\xi_t + Re\left(F\xi_r + \frac{G\xi_\theta}{r} - F_z v_r + G_z u_r - wG_{zz}\right) + Ro\left(H\xi_z + H_z\xi - F_z v - Fv_z - 2G_z u - 2Gu_z + \frac{Fw_\theta}{r} + G_z u\right) - Cou_z = \nabla^2\xi - \frac{v_z}{r^2} - \frac{2u_{\theta z}}{r^2} \tag{8a}$$

$$\eta_t + Re\left(F\eta_r + \frac{G\eta_\theta}{r} - \frac{F_z v_\theta}{r} + \frac{G_z u_\theta}{r} + wF_{zz}\right) + Ro\left(H_z\eta + H\eta_z + F_z u + Fu_z - 2G_z v - 2Gv_z - Fw_r - \frac{Gw_\theta}{r} - F_z u + \frac{Gw_\theta}{r}\right) - Cov_z = \nabla^2\eta - \frac{u_z}{r^2} - \frac{2v_{\theta z}}{r^2}, \tag{8b}$$

To adopt a local rectangular coordinate system centered at some fixed value of Re let $dr \rightarrow dx$ and $rd\theta \rightarrow dy$. The viscous terms $1/r$ and $1/r^2$ have been omitted because $1/r = -1/Re$. The rectangularized horizontal component of vorticity equations derived from Eqs. (8a, b), are then

$$\xi_t + Re(F\xi_x + G\xi_y - F_z u_x + G_z u_x - G_{zz} w) + Ro(H\xi_z + H_z\xi - F_z v - Fv_z - 2G_z u - 2Gu_z + Fw_y + G_z u) - Cou_z = \nabla^2\xi \tag{9a}$$

$$\eta_t + Re(F\eta_x + G\eta_y - F_z v_y + G_z u_y + F_{zz} w) + Ro(H_z\eta + H\eta_z + F_z u + Fu_z - 2G_z v - 2Gv_z - Fw_x - Gw_y - F_z u + Gw_y) - Cov_z = \nabla^2\eta \tag{9b}$$

The two pairs of Eqs. (7a, b) and (9a, b) are now rotated through an angle $\delta = \varepsilon + \pi/2$ as illustrated in Fig. 3, where ε is the angle of the new $\hat{x}$ axis with respect to the tangential direction. The instabilities are assumed to be 2-dimensional vortices independent of new $\hat{x}$-direction, so in the rotated equations $\partial/\partial\hat{x} = 0$.

The stream function for the flow in the new $(\hat{y},\ \hat{z})$-plane is defined by

$$w = \frac{\partial\phi}{\partial y},\ v = -\frac{\partial\phi}{\partial z},\ \xi = \nabla^2\phi \tag{10}$$

where $\hat{}$ is deleted for convenience.

The perturbation velocity u and stream function ϕ may be assumed as

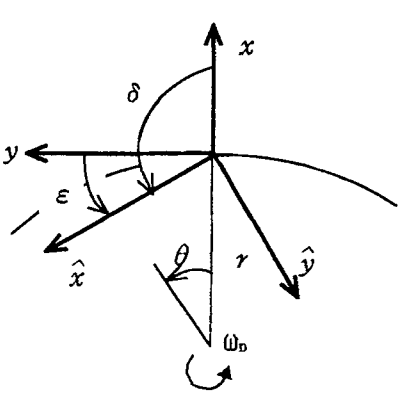

Fig. 3 Rotation system

$$u(y, z, t)=U(z)\exp[i(\bar{k}y-\bar{\beta}t)],$$
$$\phi(y, z, t)=\Phi(z)\exp[i(\bar{k}y-\bar{\beta}t)] \quad (11a)$$

The dimensional wave number $\bar{k}$ and wave frequency $\bar{\beta}$ are nondimensionalized as

$$k=\bar{k}D,$$
$$\beta=\frac{\bar{\beta}}{\omega_D} \quad (11b)$$

where the ratio β/k is referred to the wave velocity Cp.

The reoriented equations with expression of Eqs. (10)-(11) are

$$U''-RoHU'+[i\beta+Re(FC+GS)ik-(Ro\ F+K^2)]U-(2Ro\ G+Co)\Phi'-Reik(-F'S+G'C)\Phi=0 \quad (12a)$$

$$\Phi''''-RoH\Phi'''+[i\beta+Re(FC+GS)ik-(RoH'+RoF+2k^2)]\Phi''-Ro[F'-Hk^2-C(F'C+G'S)]\Phi'-[i\beta k^2+Re(FC+GS)ik^3+Re(F''C+G''S)ik+RoH'k^2+Rok^2S(FS-GC)+Ro\ k^2C(GC-FS)+k^4]\Phi+(2Ro\ G+Co)U'-Ro[S(F'C+G'S)-2G']U=0 \quad (12b)$$

where $C=\cos\varepsilon$, $S=\sin\varepsilon$. The corrected sign term is $(GC-FS)$ and the whole convective terms $Ro(F'C+G'S)\Phi'$, $RoS(F'C+G'S)U$ and $Rok^2S(FS-GC)$ are included.

In order to specify the problem completely, boundary conditions are applied to the eigenfunction $(U(\eta), \Phi(\eta))$. Evidently, the velocity disturbances quantities u, v and w must be zero at the rotating disk surface and at a large distance out $(\eta\rightarrow\infty)$. Therefore, the nondimensional boundary conditions are:

$$U(0)=\Phi(0)=\Phi'(0)=0,$$
$$U'(\infty)=\Phi(\infty)=\Phi''(\infty)=0. \quad (13)$$

The reformulated stability Eqs. (12a, b) with boundary conditions (13) are complex-valued, 6th-order, linear system of homogeneous differential equations.

2.3 Numerical method

The boundary value problem (12a, b) and (13) can be solved by using a technique of simple shooting from $\eta=\eta_\infty$, where it is the asymptotic solution valid as $\eta\rightarrow\infty$, to $\eta=0$, and one seeks to satisfy the conditions in (13) that apply at $\eta=0$ (Hwang, 1996). Also, this problem can be solved by using the finite difference method adopted the Adams-Bashforth time-step, centered difference in z as did Faller (1991). To reduce the error propagation and to avoid the inaccuracies in both methods, the orthogonal collocation method is employed to solve the problem. Thus, our results were obtained primarily by using a two-point boundary value problem code COLNEW that was based upon the adaptive orthogonal collocation method using B-spline. For the approximation of η_∞ in Eq. (13), $\eta_\infty=40-120$ was chosen, that was the same value for the base flow.

To generate the families of solutions, an *ad hoc* scheme was used as described below. Since there is no simple way to normalize the solutions of the eigenvalue problem (12a, b) and (13) which has all homogeneous boundary conditions, an alternative must be found to avoid the trivial solution.

The boundary conditions (13) are modified slightly but significantly. These conditions are expressed in the real and imaginary parts,

$$U_R(0)=U_I(0)=\Phi_R(0)=\Phi_I(0)=0,$$
$$|\Phi_R''(0)|=|\Phi_I''(0)|=J,$$
$$U_R'(\infty)=U_I'(\infty)=\Phi_R(\infty)=\Phi_I(\infty)=\Phi_R''(\infty)=\Phi_I''(\infty)=0 \quad (14)$$

with $10^{-3}\leq|J|\leq10^{-1}$.

The computing procedure employed to use the orthogonal collocation code COLNEW for obtaining the neutral stability curve is quite similar to that employed in the simple shooting. For a given value Re, one guesses a pair of eigenvalues k and β. One then solves the linear stability Eqs. (12a, b) with the modified boundary conditions (14), replacing $\Phi'(0)=0$, using COLNEW, and iterates by adjusting the values of k and β until the boundary conditions $\Phi_R'(0)=\Phi_I'(0)=0$ are satisfied with $|\Phi_R'(0)|+|\Phi_I'(0)|\leq10^{-6}$.

In our calculation, the following criteria was used to get the acceptable solution.

$$\min_{0\leq\eta\leq\infty}\left(\frac{|\Phi_R'(0)|}{|\Phi_R'(\eta)|}, \frac{|\Phi_I'(0)|}{|\Phi_I'(\eta)|}\right)\leq10^{-4} \quad (15a)$$

$$\max\left(\frac{|\Phi_R'(0)|}{M}, \frac{|\Phi_I'(0)|}{M}\right)\leq10^{-7} \quad (15b)$$

where M was maximum value of the eigenvector components (*i.e.*, U, U', Φ, Φ', Φ'') on $0 \leq \eta \leq \eta_\infty$.

In addition, the error estimates given by COLNEW were less than 10^{-5}.

3. Results and Discussion

Since there is one neutral stability curve corresponding to each of two instability modes, two critical Reynolds numbers are considered. These Reynolds numbers $Re_{c,1}$ and $Re_{c,2}$ are the smallest Reynolds numbers on the neutral stability curve corresponding to Type I instability and Type II instability in stability planes, respectively (see Fig. 4). For $Re < Re_{c,i}$, $(i=1, 2)$ any small disturbance of Type i instability mode decays, whereas for $Re > Re_{c,i}$ at least some disturbances of Type i mode are amplified.

The instability that appears in the form of stationary spiral vortices at large Reynolds number and positive azimuth angle relative to circles on a disk is Type I. Whereas Type II as well as Type I has a form of spiral vortices but of the opposite angle relatively and with a lower value of Re_c, and the vortices move rapidly outward.

We obtained the stability results that satisfied the criteria for accuracy (15a, b) for several ε (the azimuth angle of disturbance wave) values in the range $-28° \leq \varepsilon \leq 17°$. Consequently, we obtained more complete 4-dimensional neutral stability curves, corresponding to the Type I and II instabilities, than the previous investigators. The calculated stability curves in the (k, Re)-, (β, Re)-, and (Cp, Re)-planes are presented in Figs. 4-7. The 4-dimensional neutral stability curves in Fig. 4 were drawn by connecting the most outer portions of stability curves from Figs. 5-7. The flow is unstable in the inner region of these 4-dimensional curves.

As seen from Fig. 4, the upper part of the neutral stability curve in the (k, Re)-plane is expected to be bounded by the value of $k=0.75$ near $Re=1200$. In other words, the flow is always stable for the disturbance whose wave number, in terms of k, is greater than 0.75. The physical wave number corresponding to $k=0.75$ is $\bar{k}=4.27\text{cm}^{-1}$ if $\omega_D=0.325$ rps.

From the two neutral stability curves in Fig. 4, it can be found that the Type I and II instabilities have distinctive stability characteristics. If we consider Type II instability, the flow becomes first unstable, at early stage of instability, for some disturbances, for example, those which are in a band of wave numbers $0.0 \lesssim k \lesssim 0.587$ with wave speeds $15.7 \leq Cp \leq 270$ and with azimuth

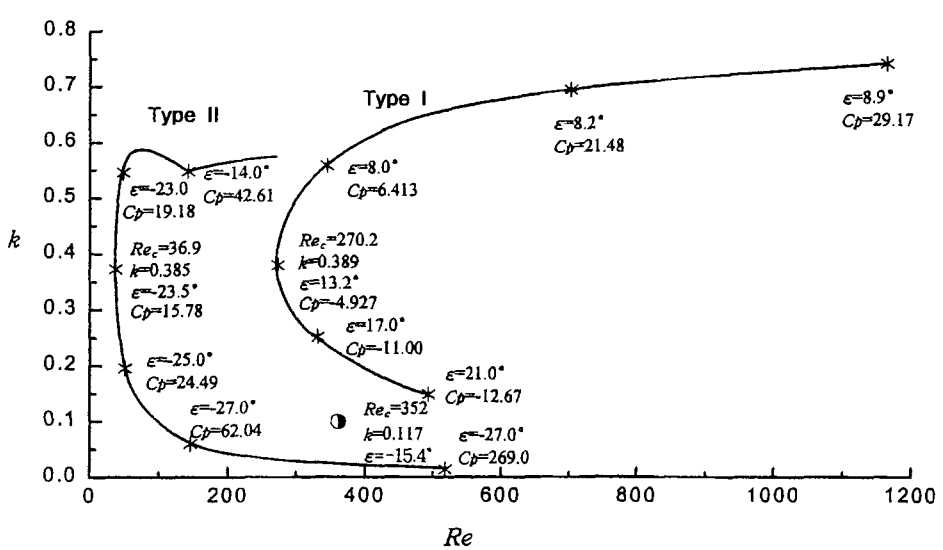

Fig. 4 4-dim. neutral stability curves for the Kármán layer, corresponding to the Type I and II instabilities. The marked data from Faller (1991) (◑) corresponds to Fig. 1(a)

angles $-28.4° \leq \varepsilon \leq -14°$. Also, if we consider Type I instability, the flow becomes first unstable for some disturbances in $0.15 \leq k \leq 0.747$ with $-12.6 \leq Cp \leq 29.1$ and with $8.2° \leq \varepsilon \leq 21°$. The Type I as well as Type II instabilities have a form of spiral vortices. The disturbances of Type I mode, in contrast with those of Type II mode, can be considered as almost stationary waves due to their relatively small values of Cp.

Some disturbance of Type II mode can be quickly amplified from the position of relatively small $Re_{c,2}$ as it travels spirally outward with high wave speed and with the opposite angle relative to circle on the disk in Fig. 3. The Type II amplification data of Faller (1991) corresponding to Fig. 1(a) is shown as the mark (◑) in Fig. 4. The amplified disturbances of $k=0.117$ with $\varepsilon = -15.4°$ are detected at $Re=352$, which is 10 times of our $Re_{c,2}$ downstreams. The above experimental data exists in our computed unstable region of Type II mode (see Fig. 4).

A comparison of our computed value of critical Reynolds number $Re_{c,1}$ with the respective values of previous investigators is shown in Table 1. Also, the present numerical values of critical parameters, corresponding to both the Type I and II instabilities, are compared with those of Faller (1991) and of Malik *et al.* (1981) in Table 2. The numerical results of the present work differ considerably with those obtained by Faller (1991). However, both results are agreed well within resonable limits, not only considering the terms of linear stability equations he formulated were different with those of the present work, but the numerical techniques he employed were not as powerful as those available to the authors.

From the evidence provided by the hot-wire measurements of Wilkinson and Malik (1985) and of Kobayashi *et al.* (1980), it can be founded that the value of $Re_{c,1}$ is in the range 290 ± 20. Some numerical values of the available data for $Re_{c,1}$ are considerably different due to various modeling and numerical scheme. From the well-known, theoretical and experimental values of $Re_{c,1}$ given in Table 1, there is considerable variation of the theoretical results. The theoretical results of Brown (1959) and of Cebeci and Stewartson (1980) are considerably less than the

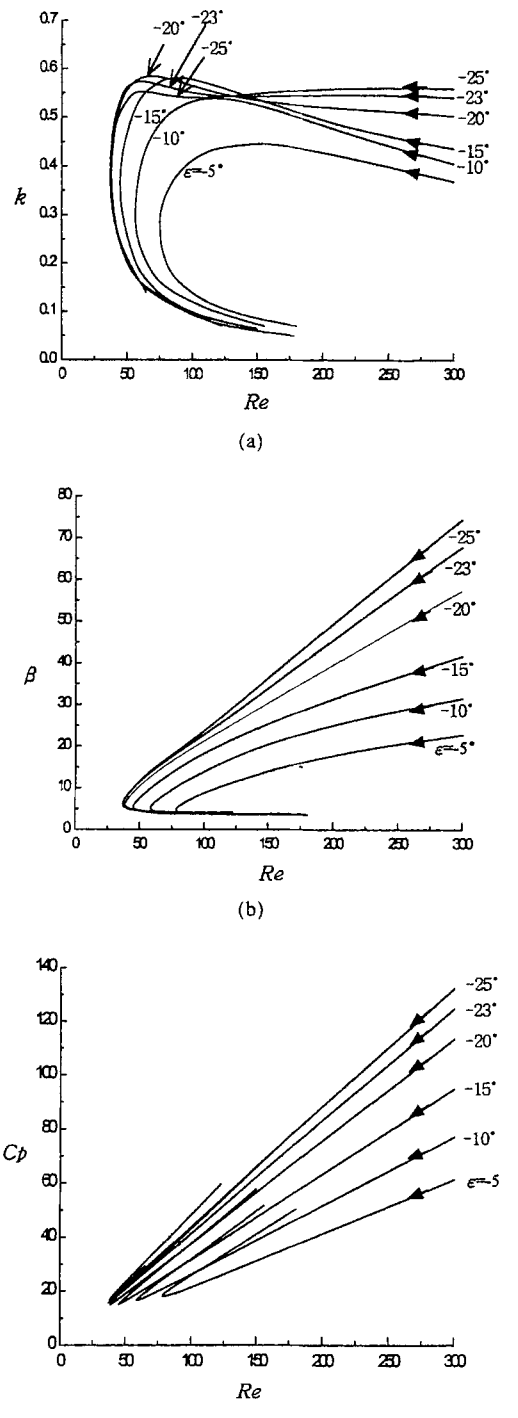

Fig. 5 Stability curves for $\varepsilon = -25°$, $-23°$, $-20°$, $-15°$, $-10°$, and $-5°$ in the (a) (k, Re)-, (b) (β, Re)- and (c) (Cp, Re)-planes

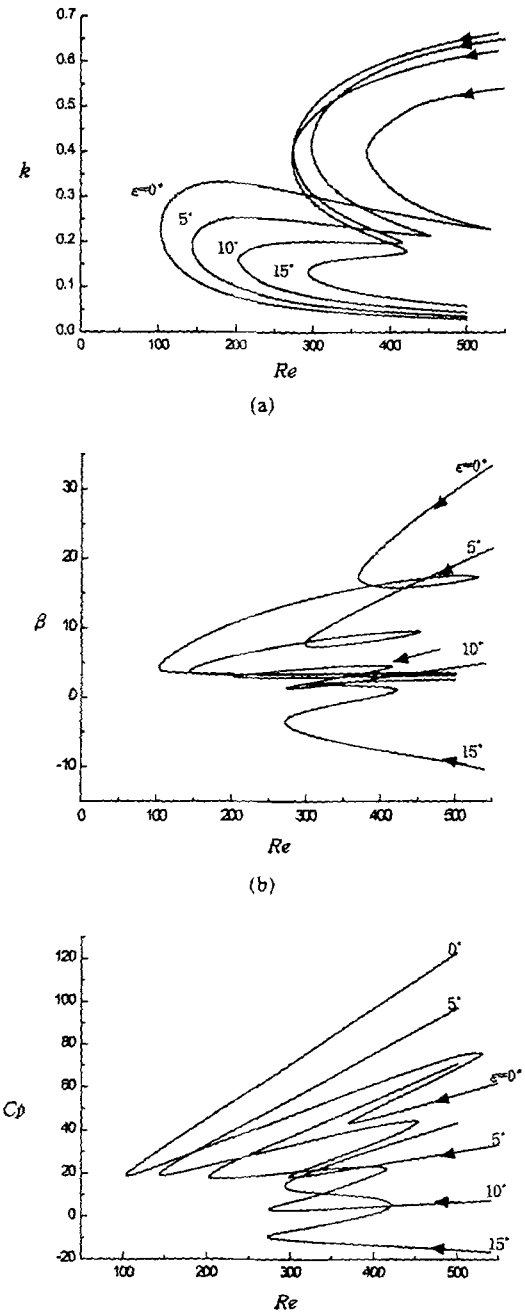

Fig. 6 Stability curves for $\varepsilon=0°$, 5°, 10°, and 15° in the (a) (k, Re)-, (b) (β, Re)- and (c) (Cp, Re)-planes

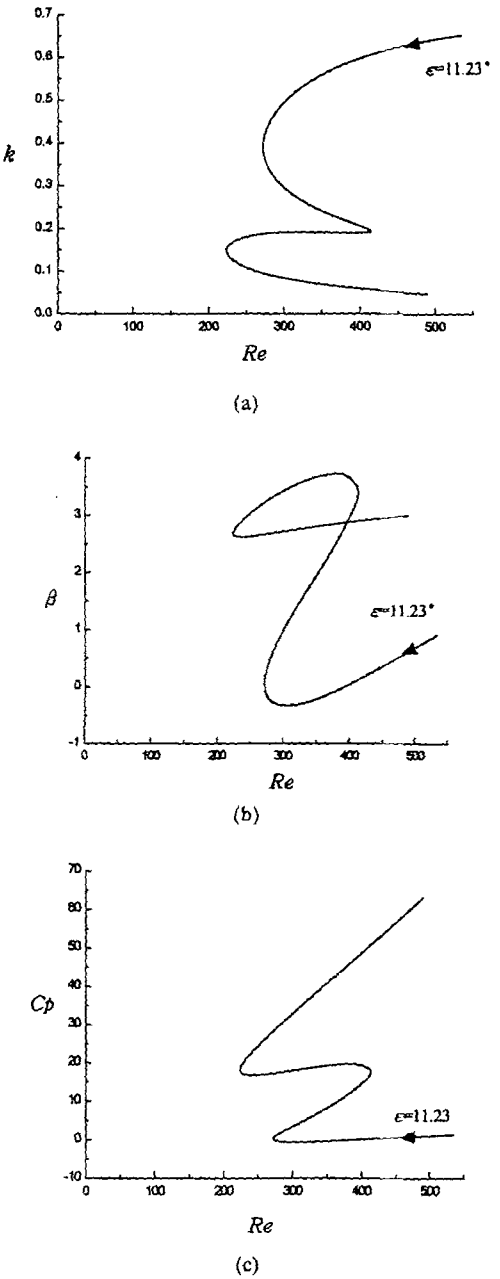

Fig. 7 Stability curve for $\varepsilon=11.23°$ in the (a) (k, Re)-, (b) (β, Re)- and (c) (Cp, Re)-planes

experimentally observed data due to neglecting the effects of Coriolis term and streamline curvature. Therefore, the theoretical value of $Re_{c,1}$ is significantly dependent upon whether these effects are included or not in the stability analysis.

The disturbance waves, corresponding to the Type I instability, are almost stationary, since the absolute values of wave speed $|Cp|$ are very small near $Re_{c,1}$. Namely, for ε in the range $9° \leq \varepsilon \leq 15°$, the value of $|Cp|$ at the lower *nose* of a

stability curve is considerably small (see Figs. 6 (c), 7(c) and, also, Table 3). Whether the disturbances are very slowly moving waves or stationary ones, they must spiral outward as does the base flow. This indicates that the value of Cp must be positive or almost zero for physical flows. The present stability results show that the flow becomes first unstable near the position of $Re_{c,1}=270.2$ for a disturbance wave of $k_{c,1}=0.389$ with $\varepsilon_{c,1}=13.2°$. (Note that Cp is positive as $\varepsilon \rightarrow 9°$, whereas Cp is negative as $\varepsilon \rightarrow 15°$; see Fig. 4 and Table 3.) Thus, it is expected that the value of ε tends to be slightly decreased from $\varepsilon=13.2°$ towards 9° as Re is further increased from $Re_{c,1}$. The above prediction reasonably agrees with the experimental data of Kobayashi *et al.* (1980).

Malik *et al.* (1981), also, observed that the wave of stationary disturbance at $Re=294$ whose azimuth angle exists in the experimental range $11° < \varepsilon < 14°$ (Gregory *et al.*, 1955, Kobayashi *et al.*, 1980). However, our computed critical values for stationary disturbances are $\varepsilon=11.2°$, $Re=271.5$ and $k=0.40$, respectively. Evidently, our prediction for the stationary instability reasonably agrees with the previous experimental data.

Figures 8 and 9 show the eigenvector compo-

Table 1 Theoretical and experimental critical Reynolds number of Type I instability

Theoretical Results			Experimental Results		
Investigators	Critical	Method	Investigators	Critical	Method
Brown (1959)	178	Temporal instability theory	Smith (1946)	460	Hot-wire Probe
Cebeci and Stewartson (1980)	175.6	Spatial stability theory	Gregory *et al.* (1955)	430	China-clay tech.
Kobayashi *et al.* (1980)	261	Predictor-corrector Technique	Gregory and Walker (1960)	367	Acoustical slotted disk
Malik *et al.* (1981)	287	Spectral method by Chebyshev polynomials	Kobayashi *et al.* (1980)	297	Hot-wire Probe
Malik (1986)	285.36	LU factorization	Malik *et al.* (1981)	294	Hot-wire Probe
Faller (1991)	285.3	Adams-Bashforth time stepping			
Lingwood (1997)	507	Absolute instability			
Present	270.2	Orthogonal collocation and multiple shooting			

Table 2 Critical values of Type Ⅰ and Ⅱ Instabilities

Mode	Type Ⅰ		Type Ⅱ		
	Faller (1991)	Present	Faller (1991)	Malik *et al.* (1981)	Present
Re	285.3	270.2	69.4	49	36.9
k	0.378	0.389	0.279	–	0.385
ε	13.9	13.2	−19.0	–	−23.5
Cp	–	−4.927	–	–	15.78

Table 3 Data corresponding to the lower *nose* of stability curves for several ε

ε	0°	5°	9°	10°	11.2°	12°	13°	13.2°	14°	15°
$Re_{n,1}$	369.64	297.4	276.14	273.55	271.53	270.86	270.24	270.23	270.39	272.16
$Cp_{n,1}$	43.37	18.77	6.08	3.30	0.0	−2.01	−4.41	−4.93	−6.81	−9.69
k	0.40	0.40	0.40	0.40	0.40	0.40	0.389	0.389	0.38	0.40

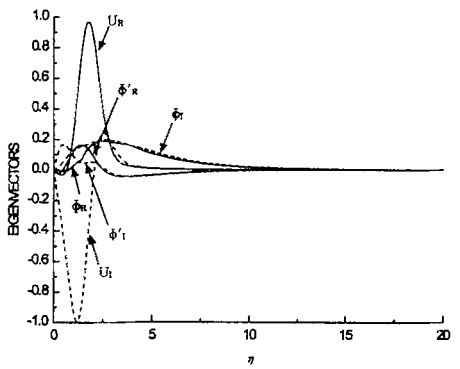

Fig. 8 Plots of eigenvector components vs. η corresponding to the Type Ⅰ instability at $Re=270.2$, $k=0.389$, $\varepsilon=13.2°$ and $\eta_\infty=20$

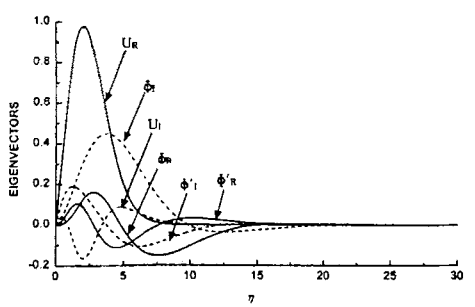

Fig. 9 Plots of eigenvector components vs. η corresponding to the Type Ⅱ instability at $Re=36.9$, $k=0.385$, $\varepsilon=-23.5°$ and $\eta_\infty=40$

nents (U_R, U_I, Φ_R, Φ'_R, Φ_I, Φ'_I) which satisfy the accuracy criteria (15. a, b), corresponding to two *noses* of neutral stability curves at $Re_{c,1}$ and $Re_{c,2}$. In these figures, the eigenvectors are normalized by the maximum value of the components. The shapes of the components of the eigenvectors change drastically as $k \cdot Re$ increases.

4. Conclusions

The hydrodynamic instability of the Kármán boundary-layer flow has been numerically investigated by employing the linear stability theory. The previously known stability equations of Faller (1991) are reformulated by correcting the sign error and by keeping the whole convective terms. The reformulated stability equations are accurately solved by a two-point boundary-value problem solving code. A computer code COLNEW, based on the orthogonal collocation is used for obtaining the neutral stability curve. The results include more complete 4-dimensional neutral stability curves corresponding to the Type Ⅰ and Ⅱ instabilities. The present stability equations are slightly different with those of Faller (1991), but our obtained results, in particular, on Type Ⅱ instability are considerably different. However, both results agree within reasonable limit, considering both of characteristic shapes of neutral stability curves are almost same.

The results show that the flow is always stable for the disturbance whose wave number $k>0.75$. The first unstable condition for Type Ⅱ instability mode is the band of wave numbers $0.0 \lesssim k \lesssim 0.587$ with azimuth angles $-28.4° \lesssim \varepsilon \lesssim -14°$. Also, the similar condition for Type Ⅰ instability mode is $0.15 \lesssim k \lesssim 0.747$ with $8.0° \lesssim \varepsilon \lesssim 21°$. These obtained two stability results are rather more complete and they have relatively lower values of critical Reynolds numbers than those of Faller (1991). The small disturbances intend to be decayed for $Re < Re_c$ whereas they can be selectively amplified, at least, for $Re > Re_c$.

The prediction from the present results on both instability modes excellently agrees with the previously known experimental data. In particular, it

reasonably explains the previously observed subtle phenomena of Type I instabilities by considering the relation between the disturbance wave speeds and azimuth angles.

Acknowledgements

This Paper was Supported by 63 Research Fund, Sungkyunkwan University, 1998.

References

Bader, G. and Ascher, U., 1985, "A New Basis Implementation for a Mixed Order Boundary O. D. E. Solver," *Tech. Rep.* 85-11, Dept. of Computer Science, U. of British Columbia, Vancouver, Canada.

Brown, W. E., 1959, "Numerical Calculation of the Stability of Cross Flow Profiles in Laminar Boundary Layers on a Rotating Disk and on a Swept-back Wing and an Exact Calculation of the Stability of the Blasius Velocity Profile," *Northrop Aircraft Rept.* NAI-59-5.

Cebeci, T. and Stewartson, K., 1980, "On Stability and Transition in Three-dimensional Flows," *AIAA Journal*, Vol. 18, No. 4, pp. 398~405.

Faller, A. J., Yang, S. T. and Piomelli, U., 1989, "Instability of the KEB Boundary Layers," *Tech. Note* BN-1102, Inst. Phys. Sci. and Tech., U. of Maryland.

Faller, A. J., 1991, "Instability and Transition of Disturbed Flow over a Rotating Disk," *J. Fluid Mech.*, Vol. 230, pp. 245~269.

Gregory, N. and Walker, W. S., 1960, "Experiments on the Effect of Suction on the Flow due to a Rotating Disk," *J. Fluid Mech.*, Vol. 9, pp. 225~234.

Gregory, N., Stuart, J. T. and Walker, W. S., 1955, "On the Stability of Three-dimensional Boundary Layers with Application to the Flow due to a Rotating Disk," *Phil. Trans. Roy. Soc.* Vol. 248, pp. 155~199.

Hwang, Y., 1996, "Stability of Buoyancy-Induced Flows Adjacent to a Vertical Isothermal Surface in Cold Pure Water (Neutral Stability in the Range $0 \leq R \leq 0.1515$)," *KSME J.*, Vol. 10, No. 4, pp. 498~508.

Kármán, T. von, 1921, "Über Laminare und Turbulente Reibung," *Z. Angew. Math. Mech.*, Vol. 1, pp. 233~252.

Kobayashi, R., Kohama, Y. and Takamadate, Ch., 1980, "Spiral Vortices in Boundary Layer Transition Regime on a Rotating Disk," *Acta Mechanica*, Vol. 35, pp. 71~82.

Kohama, Y. and Suda, K., 1993, "Crossflow Instability in a Spinning Disk Boundary Layer," *AIAA Journal*, Vol. 31, No. 1, pp. 212~214.

Lilly, D. K., 1966, "On the Instability of Ekman Boundary Flow," *J. of the Atmospheric Science*, Vol. 23, pp. 481~494.

Lingwood, R. J., 1997, "Absolute Instability of the Ekman Layer and Related Rotating Flows," *J. Fluid Mech.*, Vol. 331, pp. 405~428.

Malik, M. R., Wilkinson, S. P. and Orszag, S. A., 1981, "Instability and Transition in Rotating Disk Flow," *AIAA Journal*, Vol. 19, No. 9, pp. 1131~1138.

Malik, M. R., 1986, "The Neutral Curve for Stationary Disturbances in Rotating Disk Flow," *J. Fluid Mech.*, Vol. 164, pp. 275~287.

Smith, N. H., 1947, "Exploratory Investigation of Boundary Layer Oscillations on a Rotating Disk," *NACA Tech. Note* 1227.

Sparrow, E. M. and Gregg, J. L., 1960, "Mass Transfer, Flow and Heat Transfer about a Rotating Disk," *Transactions ASME, J. Heat Transfer*, Vol. 82, pp. 294~302.

Wilkinson, S. P. and Malik, M. R., 1985, "Stability Experiments in the Flow over a Rotating Disk," *AIAA Journal*, Vol. 23, No. 4, pp. 588~595.